2016

# The Global Stability of the Solution to the Morse Potential in a Catastrophic Regime

Weerapat Pittayakanchit
*Harvey Mudd College*

# The Global Stability of the Solution to the Morse Potential in a Catastrophic Regime

**Weerapat Pittayakanchit**

Andrew J. Bernoff, Advisor

Chad Topaz, Reader


**Department of Mathematics**

May, 2016

# Abstract

Swarms of animals exhibit aggregations whose behavior is a challenge for mathematicians to understand. We analyze this behavior numerically and analytically by using the pairwise interaction model known as the Morse potential. Our goal is to prove the global stability of the candidate local minimizer in 1D found in (Bernoff and Topaz, 2013). Using the calculus of variations and eigenvalues analysis, we conclude that the candidate local minimizer is a global minimum with respect to all solution smaller than its support. In addition, we manage to extend the global stability condition to any solutions whose support has a single component. We are still examining the local minimizers with multiple components to determine whether the candidate solution is the minimum-energy configuration.

# Contents

**Abstract** **iii**

**Acknowledgments** **ix**

**1 Introduction & Background** **1**

**2 Global Stability with Respect to the Perturbation inside the Support** **5**
2.1 Properties of $\mathcal{L}$ . . . . . 8
2.2 Eigenvalues of $\mathcal{L}$ are positive . . . . . 10
2.3 A Numerical Method of finding eigenvalues . . . . . 27

**3 Convex Relaxation** **29**
3.1 Periodic Boundary Condition . . . . . 33
3.2 Numerical Scheme . . . . . 35
3.3 Global Minimum with a single component . . . . . 36

**4 Conclusion and Future Work** **39**

**Bibliography** **41**

# List of Figures


1.1 The density plot of the locally stable solution in Eq. 1.7 with $G = 0.5$ and $L = 2$ . . . . . 4

2.1 Plot of the real values of $m$ and $n$ for $\lambda \in (-2(GL^2 - 1), 0) \cup \left(0, \frac{2(1-\sqrt{G})^2L^2}{L^2-1}\right)$ where $G = 0.4$ and $L = 2$. . . . . 14

2.2 Plot of the imaginary values of $m$ and $n$ for $\lambda \in (-2(GL^2 - 1), 0) \cup \left(0, \frac{2(1-\sqrt{G})^2L^2}{L^2-1}\right)$ where $G = 0.4$ and $L = 2$. . . . . 14

2.3 Plot of $f_3(m)$ and $f_4(n)$ as functions of eigenvalue $\lambda \in (-2(GL^2 - 1), 0)$ with $G = 0.7$ and $L = 2$. (Note that $m$ and $n$ are uniquely determined for each $\lambda$). . . . . 17

2.4 Plot of $g_3(m)$ and $g_4(n)$ as a function of eigenvalue $\lambda \in (-2(GL^2 - 1), 0)$ with $G = 0.7$ and $L = 2$. (Note that $m$ and $n$ are uniquely determined for each $\lambda$). . . . . 20

2.5 Plot of $F_o$ from $\lambda = 0$ to $\frac{2L^2(1-\sqrt{G})^2}{L^2-1}$ for $G = 0.4, L = 2$. The x-intercepts represent eigenvalues that satisfy the condition which means that the odd eigenfunction corresponding to that eigenvalue exist. . . . . 26

2.6 Plot of $F_e$ from $\lambda = 0$ to $\frac{2L^2(1-\sqrt{G})^2}{L^2-1}$ for $G = 0.4, L = 2$. The x-intercepts represent eigenvalues that satisfy the condition which means that the even eigenfunction corresponding to that eigenvalue exist. . . . . 26

2.7 Plots comparing eigenvalues calculated from an analytical approach to eigenvalues calculated from a numerical approach. 28

3.1 A local minimum of a non-linear function may not be a global minimum, but a local minimum of a linear function must be a global minimum. . . . . 30

3.2 The solid line is the plot of periodic Morse potential and the dashed line is the plot of Morse potential. The parameter $G = 0.4$, $L = 2$, and $h = 5$. . . . . 35
3.3 Comparison between the $P$ from linear programming and from the auto-correlation of the candidate solution where $G = 0.5$, $L = 2$, $h = 10$, and the number of grids = 400 . . . . . 37
3.4 Relative errors of the comparison in Fig. 3.3, $\frac{P_{\text{linprog}} - P_{\text{analytic}}}{P_{\text{analytic}}}$, where $G = 0.5$, $L = 2$, $h = 10$, and the number of grids = 400 . 37

# Acknowledgments

I would like to express my gratitude to Harvey Mudd College, Macalester College, and the NSF (Grant DMS-1412674) for funding this research. I also would like to thank Andrew J. Bernoff, Rob Thompson, Chad Topaz, and Ivan Ventura for their great advice and support. Last but not least, I thank Zhaoqi Li for his partnership during the summer of 2015 at Macalester College.

# Chapter 1

# Introduction & Background

Swarming is a collective behavior that animals such as fish, birds, sheep, or insects exhibit when they move together. Biologists found that fish react to other fish in the same species attractively if they are too close and repulsively if they are far away (Breder, 1954). Other study shows that this type of short-ranged repulsive and long-ranged attractive interactions can generalize to other animals (Eftmie et al., 2007). Animals can sense each other via seeing, smelling, hearing, touching, or through chemical signals. They can acknowledge the positions of other animals and adjust their positions accordingly as if there is a invisible force that keeps them together. Mathematicians and biologists model this as a "social force" that governs pairwise interactions between animals.

There are many mathematical models describing social forces but the subject of our interest is the Morse potential model which is used frequently in the literatures (Bernoff and Topaz, 2013; Leverentz et al., 2009; Mogilner et al., 2003; d'Orsogna et al., 2006). The Morse potential is defined to be

$$Q(z) = e^{-z} - GLe^{-z/L} \tag{1.1}$$

where $z$ represents a distance between two animals, while $G$ and $L$ are the relative strength and length scale of attraction to repulsion respectively. $G < 1$ means that the attraction is weaker than the repulsive part at short distance. $L > 1$ means that the length scale of the attraction is longer than the repulsion. The negative gradient of the Morse potential is the social force:

$$F(z) = \hat{z}(e^{-z} - Ge^{-z/L}) \tag{1.2}$$

where $\hat{z}$ is the unit vector pointing from the source toward the target. When $G < 1$ and $L > 1$, the Morse potential model captures the characteristic of

the force between animals that is short-ranged repulsive and long-ranged attractive.

The social force differs from the force defined in classical mechanics, in which the acceleration is proportional to the force, $\vec{F} = m\vec{a}$. A social force is the force between biological organism and is a pseudo force created to explain the swarming phenomena. Instead of acceleration, the velocity of each animal is proportional to the amount of force acting on it (Bernoff and Topaz, 2013; Mogilner and Yang, 1999). The velocity of particle $i$ is

$$\vec{v}_i = \frac{\partial}{\partial t}\vec{x}_i = \sum_{j=1, j\neq i}^{N} \vec{F}(|\vec{x}_i - \vec{x}_j|) = \sum_{j=1, j\neq i}^{N} \vec{F}_{ij}$$

where $\vec{x}_i$ is the position of particle $i$ and $\vec{F}_{ij}$ is the forces from particle $j$ acting on particle $i$. Some swarming model uses a discrete approach where animals are viewed as a point particle. We can easily simulate this model, as it is similar to molecular dynamics simulation. Nevertheless, it is hard or even impossible to analyze. For a system of $N$ particles in $n$ dimensions, we have $N$ differential equations involving $nN$ degrees of freedom describing the position of each particle. There currently is no study which takes this approach and solves a steady state solution describing positions of each particle analytically. However, when $N$ is large, we can approximate the problem in a continuum regime. The problem becomes more tractable if we do not consider the positions of animals directly but think of them as a density distribution function $\rho$. This method is well studied using aggregation equations (Bodnar and Velasquez, 2005, 2006; Bernoff and Topaz, 2013). In 1D, we can write the aggregation equation as

$$\rho_t + (\rho V)_x = 0, \qquad V(x) = \int_{\mathbb{R}} F(x-y)\rho(y)dy \tag{1.3}$$

where $V$ is the velocity field obtained from the convolution with the social force $F$ as in Eq. 1.2. In a continuum model, it is straightforward to show that the total energy due to internal interactions is

$$W = \frac{1}{2}\int_{\Omega}\int_{\Omega} \rho(x)\rho(y)Q(x-y)dxdy. \tag{1.4}$$

where $\Omega$ is a domain of the problem and $Q$ is the Morse potentitial associated with the Morse interaction force $F$:

$$Q(z) = -\int_{-\infty}^{z} F(x)dx = e^{-z} - GLe^{-z/L} \tag{1.5}$$

After taking the time derivative of Eq. 1.4, the rate of energy dissipation can be described as:

$$\frac{d}{dt}W(\rho) = -\int_{\Omega} \rho(x)V(x)^2 dx. \tag{1.6}$$

Since the density distribution function cannot be negative, the energy will dissipate as long as $V$ is not uniformly zero in $\Omega$. Thus, the stable equilibrium states $V = 0$ corresponds to the minimizer of $W$ (Leverentz et al., 2009).

In 1D, the studies of (Leverentz et al., 2009; Bernoff and Topaz, 2013) find the steady state corresponding to the minimizer of $W$ using moment generating functions and calculus of variations to show four different dynamical regimes in the parameter space of $G$ and $L$:

1. $G > 1$ and $L < 1$: in this parameter space, the attaction force is purely attractive. As a result, particles are pulled together and form a single delta function at the center of mass of the system.

2. $G > 1$ and $L > 1$: in this parameter space, the Morse interaction forces exhibits long-ranged repulsion and short-ranged attraction. As a result, particles form separate delta functions, and the number of delta functions in the steady state depends on the starting positions.

3. $G < 1$ and $G < 1/L^2$: this parameter space correspond to the H-stable system. The study in (Leverentz et al., 2009) shows that the swarm spreads indefinitely and its steady state solution is the state of uniform density, which can be reached if the space of the solution is bounded. The global stabilty of the solution is throughly understood.

4. $G < 1$ and $G > 1/L^2$: this parameter space corresponds to the catastrophic regime of Morse potential model. The study of (Bernoff and Topaz, 2013) finds a locally stable solution (see Fig. 1.1),

$$\bar{\rho}(x) = \begin{cases} C\cos(\bar{\mu}x) + D & , x \in \Omega_{\bar{\rho}} = [-H, H] \\ 0 & , \text{Otherwise} \end{cases} \tag{1.7}$$

   but the global stability has not been proved.

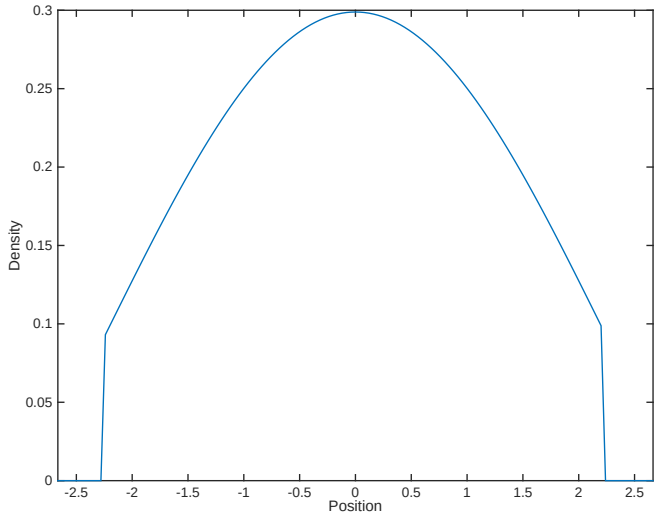


**Figure 1.1** The density plot of the locally stable solution in Eq. 1.7 with $G = 0.5$ and $L = 2$

The parameters in Eq. 1.7 are

$$\bar{\mu} = \sqrt{\frac{GL^2 - 1}{L^2(1-G)}},$$

$$H = \frac{1}{\bar{\mu}} \cot^{-1}_{[0,\pi]} \left\{ \frac{GL - 1}{\sqrt{(1-G)(GL^2-1)}} \right\},$$

$$C = \frac{M}{2(H+L+1)} \frac{\sqrt{G}(L^2-1)}{L(1-G)},$$

$$D = \frac{M}{2(H+L+1)}.$$

Mathematicians are interested in the catastrophic regime of Morse potential model because in this parameter space the Morse interaction force exhibits short-ranged attraction and long-ranged repulsion and the steady state forms a non-trivial density distribution. As mentioned, the global stability of this solutions has not been proved and it is mathematically challenging to do so. This senior thesis intends to study and prove the global stability of the locally stable solution in Eq. 1.7.

# Chapter 2

# Global Stability with Respect to the Perturbation inside the Support

A local minimizer is the steady state of the system, in which a small perturbation increase the energy, so the system is in stable equilibrium. Nevertheless, a local minimizer may not be a global minimizer, that is a large perturbation may decrease the energy and destabilize the system. We would like to show that the candidate solution found in (Bernoff and Topaz, 2013) is a global minimizer. To acheive this, we need to show that any valid perturbation on the candidate solution increases the energy of the system. The rough plan for solving this problem is to find a corresponding eigenvalue problem and prove that the corresponding operator is positive definite.

Let's remind ourselves that the energy of the system is

$$W = \frac{1}{2}\int_\Omega\int_\Omega \rho(x)\rho(y)Q(x-y)dxdy. \tag{2.1}$$

Now, let's perturb the candidate solution $\bar{\rho}$ with a perturbing density $\widetilde{\rho}$:

$$\rho = \bar{\rho} + \epsilon\widetilde{\rho}. \tag{2.2}$$

subjected to the constraints that

$$\begin{aligned} M &= \int_\Omega \bar{\rho}(x)dx, \\ 0 &= \int_\Omega \widetilde{\rho}(x)dx, \\ 0 &\leq \bar{\rho} + \epsilon\widetilde{\rho} \end{aligned}$$

Substitute Eq. 2.2 in Eq. 2.1. We obtain:

$$W[\rho, \rho] = \frac{1}{2}W_0[\bar{\rho}, \bar{\rho}] + \epsilon W_1[\bar{\rho}, \widetilde{\rho}] + \frac{\epsilon^2}{2}W_2[\widetilde{\rho}, \widetilde{\rho}] \tag{2.3}$$

where

$$\begin{aligned} W_0[\bar{\rho}, \bar{\rho}] &= \int_\Omega \int_\Omega \bar{\rho}(x)\bar{\rho}(y)Q(x-y)\, dx\, dy \\ W_1[\bar{\rho}, \widetilde{\rho}] &= \int_\Omega \int_\Omega \bar{\rho}(x)\widetilde{\rho}(y)Q(x-y)\, dx\, dy \\ W_2[\widetilde{\rho}, \widetilde{\rho}] &= \int_\Omega \int_\Omega \widetilde{\rho}(x)\widetilde{\rho}(y)Q(x-y)\, dx\, dy \end{aligned}$$

To find the density $\bar{\rho}$ that locally (small $\epsilon$) minimizes the energy $W$, the authors of Bernoff and Topaz (2013) consider two classes of perturbing functions: one whose support stays in $\Omega_{\bar{\rho}}$, the support of the solution $\bar{\rho}$, and another whose support is the whole space $\Omega$. The local minimizer of $W$ corresponds to the density $\bar{\rho}$ which makes $W_1 = 0$ for the perturbation in $\Omega_{\bar{\rho}}$ and makes $W_1 \geq 0$ for the perturbation in $\Omega$ Bernoff and Topaz (2013). To show that the local minimizer in Eq. 1.7 is also the global minimizer, we need to further show that it satisfies $W_2 > 0$ for the perturbation in $\Omega$. We will first analyze and show that $W_2 > 0$ for the perturbation in $\Omega_{\bar{\rho}}$ and expand on that result to prove that $W_2 > 0$ for the perturbation in $\Omega$.

$$W_2[\widetilde{\rho}, \widetilde{\rho}] = \int_\Omega \int_\Omega \widetilde{\rho}(x)\widetilde{\rho}(y)Q(x-y)\, dy\, dx$$

is always greater than zero. Here, we observe that

$$W_2[\widetilde{\rho}, \widetilde{\rho}] = \int_\Omega \widetilde{\rho}(x)\mathcal{L}_0\widetilde{\rho}(x)\, dx$$

where the operator $\mathcal{L}_0$ is defined as

$$\mathcal{L}_0\widetilde{\rho}(x) = \int_\Omega \widetilde{\rho}(y)Q(x-y)\,dy.$$

Since the perturbing density $\widetilde{\rho}$ is subjected to the zero mass condition $\int_\Omega \widetilde{\rho}(x)\,dx = 0$, we want the image of our operator to be a space of zero mean function on $\Omega_{\tilde{\rho}}$. Let's define a new operator $\mathcal{L}$ as:

$$\mathcal{L}\widetilde{\rho} = \mathcal{L}_0\widetilde{\rho} + \mu = \int_\Omega \widetilde{\rho}(y)Q(x-y)\,dy + \mu$$

for some constant $\mu$ such that $\int_\Omega \mathcal{L}\widetilde{\rho}\,dx = 0$. By this definition, we derive

$$\mu = -\frac{1}{|\Omega|}\int_\Omega \tilde{\rho}(y)\left(\int_\Omega Q(x-y)\,dx\right)\,dy = -\frac{1}{|\Omega|}\int_\Omega \widetilde{\rho}(y)\widetilde{Q}(y)\,dy$$

where

$$\begin{aligned}\widetilde{Q}(y) &= \int_\Omega Q(x-y)\,dx = \int_{\Omega_{\tilde{\rho}}} Q(x-y)\,dx \\ &= \int_{-H}^{H}\left(e^{-|x-y|} - GLe^{-|x-y|/L}\right)\,dx \\ &= 2(1-GL^2) - 2e^{-H}\cosh(y) + 2GL^2e^{-H/L}\cosh(y/L).\end{aligned}$$

Using the condition $\int_\Omega \widetilde{\rho}(x)dx = 0$, we can manipulate $W_2$ to show that

$$\begin{aligned}W_2 &= \int_\Omega \widetilde{\rho}(x)\mathcal{L}_0\widetilde{\rho}(x)\,dx \\ &= \int_\Omega \widetilde{\rho}(x)\mathcal{L}_0\widetilde{\rho}(x)\,dx + \mu\int_\Omega \widetilde{\rho}(x)\,dx \\ &= \int_\Omega \widetilde{\rho}(x)(\mathcal{L}_0\widetilde{\rho}(x)+\mu)\,dx \\ &= \int_\Omega \widetilde{\rho}(x)\mathcal{L}\widetilde{\rho}(x)\,dx.\end{aligned}$$

We can write $W_2$ as the $L^2$-inner product of $\widetilde{\rho}$ and $\mathcal{L}\widetilde{\rho}$ on $\Omega$

$$W_2 = \int_\Omega \widetilde{\rho}(x)\mathcal{L}\widetilde{\rho}(x)\,dx = \left\langle\widetilde{\rho}, \mathcal{L}\widetilde{\rho}\right\rangle.$$

## 2.1 Properties of $\mathcal{L}$

Before we show that all eigenvalues of $\mathbb{L}$ are positive, we want to show that $\mathbb{L}$ is compact, self-adjoint, and has a mapping such that it sends an even function to an even function and an odd function to an odd function. Proving that $\mathcal{L}$ is a compact operator allows me to treat $\mathcal{L}$, an operator on an infinite-dimensional domain, as if it were an operator on a finite-dimensional domain. Proving that $\mathcal{L}$ is self-adjoint allows me to conclude that all eigenvalues are real, which limits the range of eigenvalues I need to search for. Last but not least, proving that $\mathcal{L}$ has a map that sends an even function to an even function and an odd function to an odd function allows me to consider even eigenfunction and odd eigenfunction separately, simplifying the problem of finding all eigenvalues.

### 2.1.1 $\mathcal{L}$ is compact

The operator $\mathbb{L}$ takes in a function and returns a function where

$$\mathcal{L}\widetilde{\rho}(x) = \int_{\Omega} \tilde{\rho}(y)\left(Q(x-y) - \frac{\widetilde{Q}(y)}{|\Omega|}\right)dy$$

for $\widetilde{Q}(y) = 2(1-GL^2) - 2e^{-H}\cosh(y) + 2GL^2e^{-H/L}\cosh(y/L)$ as found previously. $\mathbb{L}$ is an integral operator over a compact domain $\Omega = [-H, H]$ in $\mathbb{R}$. In addition, the function $Q$ and $\widetilde{Q}$ are continuous and bounded. We discussed and agreed the operator $\mathbb{L}$ can be proved as a compact operator, but I will left out the details.

### 2.1.2 $\mathcal{L}$ is self-adjointed

In a space of zero means functions, we will show that $\mathcal{L}$ is self-adjointed for the $L^2$-inner product on a bounded interval $\Omega$ containing the support of the solution $[-H, H] \subset \mathbb{R}$. Using $\rho_1$ and $\rho_2$ to represent any zero mean

functions, we write

$$\begin{aligned}
\langle \rho_1, \mathcal{L}\rho_2 \rangle &= \int_\Omega \rho_1(x)\mathcal{L}\rho_2(x)dx \\
&= \int_\Omega \rho_1(x)\mathcal{L}'\rho_2(x)dx \\
&= \int_\Omega \rho_1(x)\left(\int_\Omega Q(x-y)\rho_2(y)dy\right)dx \\
&= \int_\Omega \int_\Omega \rho_1(x)Q(x-y)\rho_2(y)dydx \\
&= \int_\Omega \int_\Omega \rho_1(x)Q(y-x)\rho_2(y)dydx \\
&= \int_\Omega \rho_2(y)\left(\int_\Omega Q(y-x)\rho_1(x)dx\right)dy \\
&= \langle \mathcal{L}\rho_2, \rho_1 \rangle .
\end{aligned}$$

This property tells us that the eigenvalues of $\mathcal{L}$ are real and eigenfunctions corresponding to distinct eigenvalues are othogonal to each other Porter and Stirling (1990).

### 2.1.3 $\mathcal{L}$ sends an even function to an even function and an odd function to an odd function

By definition, the operator $\mathcal{L}$ is

$$\mathcal{L}\widetilde{\rho}(x) = \int_\Omega \tilde{\rho}(y)\left(Q(x-y) - \frac{\widetilde{Q}(y)}{|\Omega|}\right)dy$$

Notice that

$$\begin{aligned}
\mathcal{L}\widetilde{\rho}(-x) &= \int_\Omega \tilde{\rho}(y)\left(Q(-x-y) - \frac{\widetilde{Q}(y)}{|\Omega|}\right)dy \\
&= \int_\Omega \tilde{\rho}(-y')\left(Q(x-y') - \frac{\widetilde{Q}(-y')}{|\Omega|}\right)dy' \text{ where } y' = -y
\end{aligned}$$

which implies that

1. For an even function, $\widetilde{\rho}(x) = \widetilde{\rho}(-x)$, we have $\mathcal{L}\widetilde{\rho}(-x) = \mathcal{L}\widetilde{\rho}(x)$. This indicates that $\mathcal{L}\widetilde{\rho}(-x)$ is an even function.

2. For an odd function, $\widetilde{\rho}(x) = -\widetilde{\rho}(-x)$, we have $\mathcal{L}\widetilde{\rho}(-x) = -\mathcal{L}\widetilde{\rho}(x)$. This indicates that $\mathcal{L}\widetilde{\rho}(x)$ is an odd function.

Thus, $\mathcal{L}$ maps an even function to an even function and maps an odd function to an odd function. From this, we can show that the basis of eigenfunctions can be written as a subspace of odd functions and a subspace of even functions. For any eigenfunction $\rho(x)$, we can partition it into an even part, $E(x) = \frac{1}{2}\left(\rho(x) + \rho(-x)\right)$, and an odd part, $O(x) = \frac{1}{2}\left(\rho(x) - \rho(-x)\right)$ so that

$$\rho(x) = E(x) + O(x).$$

We apply $\mathcal{L}$ to the partition of $\rho$ and obtain that

$$\begin{aligned} \mathcal{L}\rho(x) &= \mathcal{L}E(x) + \mathcal{L}O(x) \\ \lambda E(x) + \lambda O(x) &= \mathcal{L}E(x) + \mathcal{L}O(x). \end{aligned}$$

Since $\mathcal{L}E(x)$ is even and $\mathcal{L}O(x)$ is odd, both $O(x)$ and $E(x)$ have eigenvalues of $\lambda$. So we can decompose any eigenfunctions into one that is even and one that is odd.

## 2.2 Eigenvalues of $\mathcal{L}$ are positive

After we have shown the transformation of the energy minimization problem to the eigenvalue problem of $\mathcal{L}$, in this section, we will show that all eigenvalues of $\mathcal{L}$ are positive. It is easier to prove that eigenvalue $\lambda$ cannot exists in some range of value. To acheive this goal, we will divide the range of eigenvalues into 4 separated parts:

1. Eigenvalue $\lambda \notin \left(-2(GL^2 - 1), \frac{2(1-\sqrt{G})^2L^2}{L^2-1}\right)$
2. Eigenvalue $\lambda \in \left(-2(GL^2 - 1), 0\right)$
3. Eigenvalue $\lambda = 0$
4. Eigenvalue $\lambda \in \left(0, \frac{2(1-\sqrt{G})^2L^2}{L^2-1}\right)$

First, we utilize an argument on the Fourier transform of $\mathcal{L}$ to show that the eigenvalue in the region where $\lambda \notin \left(-2(GL^2 - 1), \frac{2(1-\sqrt{G})^2L^2}{L^2-1}\right)$ cannot exist. Next, we utilize inequality arguments to show that eigenvalues in

the second and third regions where $\lambda \in \left(-2(GL^2-1), 0\right)$ and $\lambda = 0$ cannot exist neither. Last but not least, we showed that there exists at least one possible eigenvalue in the region where $\lambda \in \left(0, \frac{2(1-\sqrt{G})^2L^2}{L^2-1}\right)$ using the mean value theorem. The examination in these four regions of $\lambda$ is sufficient to analytically show that $\mathcal{L}$ is a positive definite operator.

### 2.2.1 No eigenvalue exists outside of $\left(-2(GL^2-1), \frac{2(1-\sqrt{G})^2L^2}{L^2-1}\right)$

In this subsection, we will show using Fourier Transform that no eigenvalue can have value outside of $\left(-2(GL^2-1), \frac{2(1-\sqrt{G})^2L^2}{L^2-1}\right)$. By definition, any eigenfunction $\widetilde{\rho}$ of $\mathcal{L}$ can be expressed as

$$\lambda\widetilde{\rho} = \mathcal{L}\widetilde{\rho}$$

Multiply $\widetilde{\rho}$ to the left of the equation.

$$\begin{aligned}\lambda\widetilde{\rho}^2 &= \widetilde{\rho}\mathcal{L}\widetilde{\rho}\\ \lambda &= \frac{\int_\Omega \widetilde{\rho}\mathcal{L}\widetilde{\rho}\,dx}{\int_\Omega \widetilde{\rho}^2 dx}\\ &= \frac{\int_\Omega\int_\Omega \widetilde{\rho}(x)Q(x-y)\widetilde{\rho}(y)dydx}{\int_\Omega \widetilde{\rho}^2 dx}\end{aligned}$$

Since $\widetilde{\rho}$ = outside $\Omega$, we can expand the boundary of the integrations in the above equation to $(-\infty, \infty)$ without changing the values of each integration Bernoff and Topaz (2013).

$$\begin{aligned}\lambda &= \frac{\int_{-\infty}^{\infty}\int_{-\infty}^{\infty} \widetilde{\rho}(x)Q(x-y)\widetilde{\rho}(y)dydx}{\int_{-\infty}^{\infty} \widetilde{\rho}^2 dx}\\ &= \frac{1}{2\pi}\frac{\int_{-\infty}^{\infty} |\hat{\rho}(k)|^2\hat{Q}(k)dk}{\int_{-\infty}^{\infty} |\hat{\rho}(k)|^2 dk}.\end{aligned}$$

From this equation, we conclude that

$$\min_k \hat{Q}(k) \le \lambda \le \max_k \hat{Q}(k).$$

Since $Q(x) = e^{-|x|} - GLe^{-|x|/L}$, $\hat{Q}(k) = \frac{2}{1+k^2} - \frac{2GL}{1+k^2L^2}$. With simple algebra, we can show that

$$\min_k \hat{Q}(k) = \hat{Q}(0) = -2(GL^2-1)$$

and

$$\max_k \hat{Q}(k) = \hat{Q}(\frac{\sqrt{G}L^2 - 1}{L^2(1-\sqrt{G})}) = \frac{2(1-\sqrt{G})^2L^2}{L^2-1}.$$

In conclusion, we find the bound of $\lambda$ to be

$$-2(GL^2-1) \leq \lambda \leq \frac{2(1-\sqrt{G})^2L^2}{L^2-1} \tag{2.4}$$

We can slightly decrease the range even further by realizing that if $\lambda$ is equal to the extremum value then $\hat{\rho}(k) = \delta(k-\bar{k})$ where $\bar{k} = 0$ for $\lambda = -2(GL^2-1)$ and $\bar{k} = \frac{\sqrt{G}L^2-1}{L^2(1-\sqrt{G})}$ for $\lambda = \frac{2(1-\sqrt{G})^2L^2}{L^2-1}$. In the former case, $\widetilde{\rho}(x)$ = constant which violate the zero mean condition unless the constant is zero. In the latter case, $\widetilde{\rho}(x) = Ae^{i\bar{k}x} + Be^{-i\bar{k}x}$ which violates the positivity condition that $\widetilde{\rho}(x) \geq 0$ unless $A = B = 0$. The range of possible eigenvalues reduces to

$$-2(GL^2-1) < \lambda < \frac{2(1-\sqrt{G})^2L^2}{L^2-1} \tag{2.5}$$

To prove that all eigenvalues are greater than zero we need to show that there does not exist eigenfunctions corresponding to $\lambda \in (-2(GL^2-1), 0]$

### 2.2.2 Analysis for eigenvalues in the range of $\left(-2(GL^2-1), 0\right)$ and $\left(0, \frac{2(1-\sqrt{G})^2L^2}{L^2-1}\right)$

The condition for the existence on $\left(-2(GL^2-1), 0\right)$ and $\left(0, \frac{2(1-\sqrt{G})^2L^2}{L^2-1}\right)$ requires the same derivations which we will do them together in this subsection. Now, we are going to derive all possible eigenfunction of $\mathcal{L}$ via solving the integral equation corresponding to the eigenvalue problem:

$$\mathcal{L}\widetilde{\rho}(x) = \lambda\widetilde{\rho}(x) = \int_\Omega \widetilde{\rho}(y)\left(Q(x-y) - \frac{\widetilde{Q}(y)}{|\Omega|}\right)dy \tag{2.6}$$

To solve this integral equation, we apply the operator $(\partial_{xx}-1)(L^2\partial_{xx}-1)$ to both sides of the equation and obtain the differential equation:

$$\left(\lambda L^2\partial_{xxxx} + (2(1-G)L^2 - \lambda(1+L^2))\partial_{xx} + (\lambda + 2(GL^2-1))\right)\widetilde{\rho} = -\int_\Omega \widetilde{\rho}(y)\frac{\widetilde{Q}(y)}{|\Omega|}dy. \tag{2.7}$$

A particular solution for Eq. 2.7 is a constant since the right hand side is a constant. To find a homogenous solution, we plug in the ansatz $\rho = e^{m_* x}$, and obtain the quadratic equation:

$$\lambda L^2 m_*^4 + (2(1-G)L^2 - \lambda(1+L^2))m_*^2 + (\lambda + 2(GL^2 - 1)) = 0 \tag{2.8}$$

which gives a list of possible roots $m_*$ for each eigenvalue $\lambda$:

$$m_* \in \{m, -m, n, -n\}$$

where

$$\begin{aligned} m &= \sqrt{\alpha + \beta}, \\ n &= \sqrt{\alpha - \beta}, \\ \alpha &= \frac{\lambda(1+L^2) - 2L^2(1-G)}{2\lambda L^2}, \\ \beta &= -\frac{(L^2-1)\sqrt{\left(\lambda - \frac{2L^2(1+\sqrt{G})^2}{L^2-1}\right)\left(\lambda - \frac{2L^2(1-\sqrt{G})^2}{L^2-1}\right)}}{2\lambda L^2}. \end{aligned} \tag{2.9}$$

With algebraic manipulation, we can show that $m$ is real for $\lambda \in (-2(GL^2 - 1), 0)$ and pure imaginary for $\lambda \in \left(0, \frac{2(1-\sqrt{G})^2 L^2}{L^2-1}\right)$ while $n$ is pure imaginary for both $\lambda \in (-2(GL^2 - 1), 0)$ and $\lambda \in \left(0, \frac{2(1-\sqrt{G})^2 L^2}{L^2-1}\right)$. Numerical values of $m$ and $n$ for $G = 0.4$ and $L = 2$ are shown in Fig. 2.1 and 2.2.

In our interest range of $\lambda$, $m \neq n$ unless $\lambda = 0$. Thus, for $\lambda \neq 0$, the general solution of the eigenvalue equation (eq. 2.7) is a linear combination of sinh and cosh of $m$ and $n$, and a constant:

$$\widetilde{\rho}(x) = A \sinh mx + B \sinh nx + C \cosh mx + D \cosh nx + E \tag{2.10}$$

where $A, B, C, D, E \in \mathbb{C}$. The solutions to Eq. 2.7 are the solutions for Eq. 2.6, but not the other way around. The coefficients $A$, $B$, $C$, $D$, and $E$ are to be determined by the zero mass condition of the perturbing function and the conditions obtained from substituting the general solution of Eq. 2.7 back into Eq. 2.6. Since we apply the operator $(\partial_{xx} - 1)(L^2\partial_{xx} - 1)$ to solve the integral equation in Eq. 2.6, we will obtain the conditions for $A$, $B$, $C$, $D$, and $E$ from the coefficients of the mode spanned by $\{\sinh x, \cosh x, \sinh x/L, \cosh x/L\}$ which is the solution of $y$ in

$$(\partial_{xx} - 1)(L^2\partial_{xx} - 1)y = 0.$$

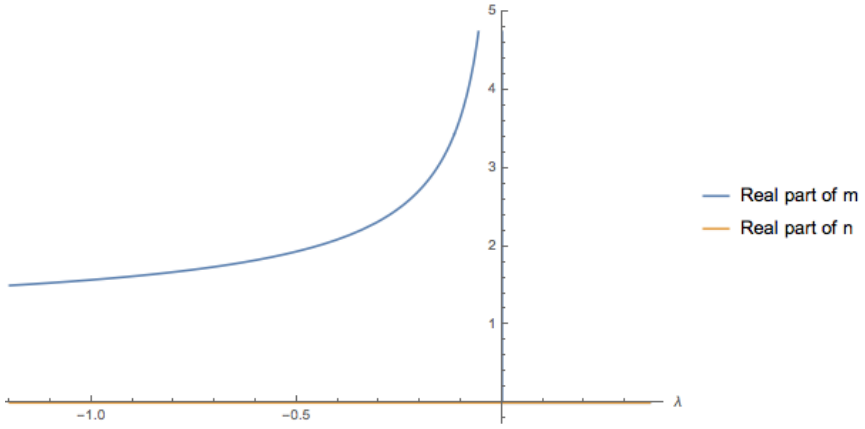


**Figure 2.1** Plot of the real values of $m$ and $n$ for $\lambda \in (-2(GL^2-1), 0) \cup \left(0, \frac{2(1-\sqrt{G})^2L^2}{L^2-1}\right)$ where $G = 0.4$ and $L = 2$.

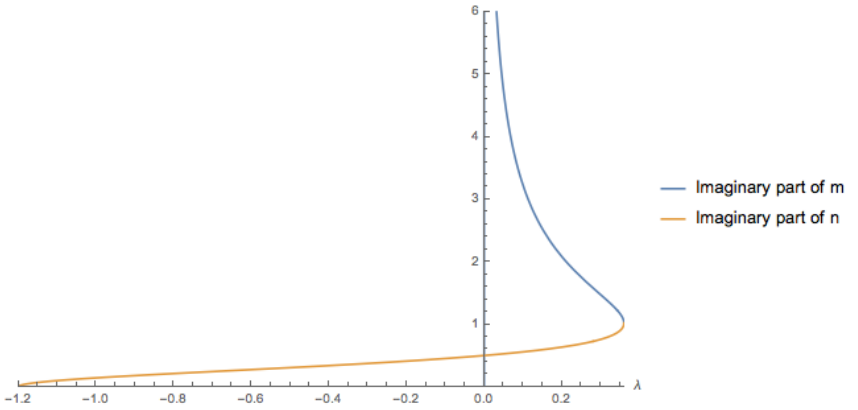


**Figure 2.2** Plot of the imaginary values of $m$ and $n$ for $\lambda \in (-2(GL^2-1), 0) \cup \left(0, \frac{2(1-\sqrt{G})^2L^2}{L^2-1}\right)$ where $G = 0.4$ and $L = 2$.

According to the property of $\mathcal{L}$ that we proved in section 2.1.3, we can analyze odd and even eigenfunctions separately. From Eq. 2.10, we claim that the odd eigenfunction is

$$\widetilde{\rho}(x) = A \sinh mx + B \sinh nx \tag{2.11}$$

and the even eigenfunction is

$$\widetilde{\rho}(x) = C\cosh mx + D\cosh nx + E. \tag{2.12}$$

For this range of $\lambda$, $\alpha$ and $\beta$ are always real. From $m = \sqrt{\alpha+\beta}$ and $n = \sqrt{\alpha-\beta}$, we can induce that $m$ and $n$ are either real or pure imaginary. It follows that $\sinh(mx)$ and $\sinh(nx)$ are odd, and $\cosh(mx)$ and $\cosh(nx)$ are even.

Next, we will develop the conditions for each eigenvalue to tell whether the eigenfunction corresponding to that eigenvalue exists. We will analyze the condition for odd and even eigenfunctions separately.

1. For odd eigenfunction, we substitute $\widetilde{\rho}(x) = A\sinh mx + B\sinh nx$ into the eigenvalue equation (Eq. 2.6) and obtain the conditions for $A$ and $B$ from the coefficients of the mode spanned by $\{\sinh x, \sinh x/L\}$ as

$$0 = \begin{bmatrix} f_1(m) & f_1(n) \\ f_2(m) & f_2(n) \end{bmatrix} \begin{bmatrix} A \\ B \end{bmatrix}$$

where

$$f_1(\zeta) = \frac{\zeta\cosh(\zeta H) + \sinh(\zeta H)}{\zeta^2 - 1}$$
$$f_2(\zeta) = \frac{\zeta L\cosh(\zeta H) + \sinh(\zeta H)}{\zeta^2 L^2 - 1}.$$

To have a nontrivial eigenfunction ($A, B \neq 0$), the determinant of the coefficient matrix must be zero:

$$0 = f_1(m)f_2(n) - f_1(n)f_2(m). \tag{2.13}$$

2. For the even eigenfunction, first, we apply the zero mass constraint to $\widetilde{\rho}(x) = C\cosh mx + D\cosh nx + E$ to obtain that

$$E = -C\frac{\sinh mH}{mH} - D\frac{\sinh nH}{nH}.$$

Next, we substitute this density function into the eigenvalue equation (Eq. 2.6) and obtain the conditions for $A$ and $B$ from the coefficients of the mode spanned by $\{\cosh x, \cosh x/L\}$:

$$0 = \begin{bmatrix} g_1(m) & g_1(n) \\ g_2(m) & g_2(n) \end{bmatrix} \begin{bmatrix} C \\ D \end{bmatrix}$$

where

$$g_1(\zeta) = \frac{\zeta H \cosh(\zeta H) + (-1 + (1+H)\zeta^2)\sinh(\zeta H)}{\zeta H(\zeta^2 - 1)}$$
$$g_2(\zeta) = \frac{\zeta H \cosh(\zeta H) + (-1 + L(L+H)\zeta^2)\sinh(\zeta H)}{\zeta H(\zeta^2 L^2 - 1)}$$

To have a nontrivial eigenfunction ($C, D \neq 0$), the determinant of the coefficient matrix must be zero:

$$0 = g_1(m)g_2(n) - g_1(n)g_2(m) \tag{2.14}$$

Finding the conditions in Eq. 2.13 and 2.14, we will prove using inequality that no eigenvalue exists in the range of $(-2(GL^2 - 1), 0)$

### 2.2.3 No Valid Eigenvalues in the range of $\left(-2(GL^2 - 1), 0\right)$

From Eq. 2.9, for this range of $\lambda$, $m$ is always greater than 1 and $n$ is an imaginary number with the value between 0 and $\bar{\mu} = \sqrt{\frac{GL^2-1}{(1-G)L^2}}$. We start our analysis to prove that no odd eigenfunction exist for these $\lambda$. To analyze Eq. 2.13, we want to group the functions of $m$ and the functions of $n$ on a separate side of the equation. So, we want to change Eq. 2.13:

$$0 = f_1(m)f_2(n) - f_1(n)f_2(m).$$

to

$$\frac{f_2(m)}{f_1(m)} = \frac{f_2(n)}{f_1(n)}$$

and in this range of $\lambda$ we found that $f_1(m) \neq 0$ and $f_1(n) \neq 0$. For convenient reasons, we will substitute $n$ with $ni$ so that we can explain functions of $n$ as functions of real number. The condition for the existence of eigenfunctions is now

$$f_3(m) = f_4(n)$$

where

$$f_3(m) = f_2(m)/f_1(m) = \frac{(m^2-1)(mL\cosh(mH) + \sinh(mH))}{(m^2L^2 - 1)(m\cosh(mH) + \sinh(mH))}$$
$$f_4(n) = f_2(in)/f_1(in) = \frac{(n^2+1)(nL\cos(nH) + \sin(nH))}{(n^2L^2 + 1)(n\cos(nH) + \sin(nH))}.$$

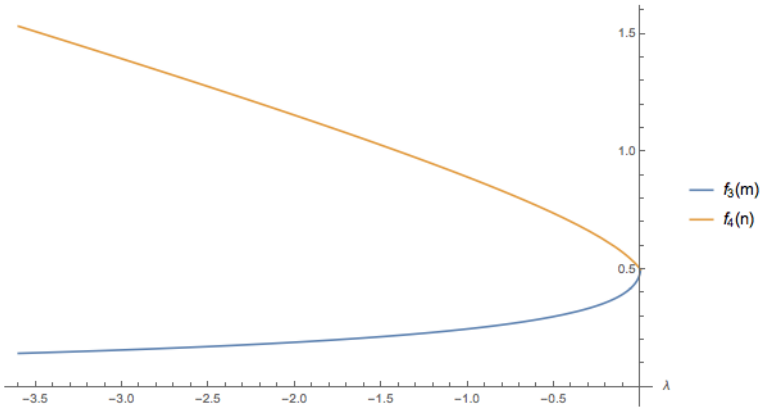


**Figure 2.3** Plot of $f_3(m)$ and $f_4(n)$ as functions of eigenvalue $\lambda \in (-2(GL^2-1), 0)$ with $G = 0.7$ and $L = 2$. (Note that $m$ and $n$ are uniquely determined for each $\lambda$).

To prove that these condition cannot be meet, we will show that $f_3(m)$ is an increasing function while $f_4(n)$ is a decreasing function for their range of $m$ and $n$, and the values of the two do not overlap. For instance, with parameter $G = 0.7$ and $L = 2$, we can plot $f_3(m)$ and $f_4(n)$ as a function of $\lambda$ in Fig. 2.3.

First, it can be easily shown that $f_3(m)$ is an increasing function when $m > 1$ because

$$f_3'(m) = \frac{(m^2-1)}{(m^2L^2-1)} \frac{(L-1)(\sinh(2mH) - 2mH)}{2(m\cosh(mH) + \sinh(mH))^2} + \frac{(mL + \tanh(mH))}{(m + \tanh(mH)} \frac{2m(L^2-1)}{(m^2L^2-1)^2}$$

and it is positive.

Next, we will show that $f_4(n)$ is a decreasing function. We write

$$f_4(n) = f_{41}(n) f_{42}(n)$$

where $f_{41}(n) = \frac{n^2+1}{n^2L^2+1}$ and $f_{42}(n) = \frac{nL\cos(nH)+\sin(nH)}{n\cos(nH)+\sin(nH)}$. So,

$$f_4'(n) = f_{41}'(n) f_{42}(n) + f_{42}'(n) f_{41}(n).$$

We find that $f'_{41}(n)$ and $f'_{42}(n)$ are negative:

$$f'_{41}(n) = -\frac{2\left(L^2-1\right)n}{\left(L^2n^2+1\right)^2}$$
$$f'_{42}(n) = -\frac{(L-1)(2Hn-\sin(2Hn))}{2(\sin(Hn)+n\cos(Hn))^2}.$$

and it is obvious that $f_{41}(n) > 0$. What left to show is that $f_{42}(n) > 0$ which will imply that $f'_4(n) < 0$. To prove $f_{42}(n) > 0$, we need to consider two separated cases of $G < 1/L$ and $G > 1/L$.

1. In the case that $G > 1/L$, since $H = \sqrt{\frac{(1-G)L^2}{GL^2-1}}\arctan_{[0,\pi]}\frac{\sqrt{(1-G)(GL^2-1)}}{GL-1}$ and $0 < n < \sqrt{\frac{GL^2-1}{(1-G)L^2}}$, we have

   $$0 < nH < \arctan_{[0,\pi]}\frac{\sqrt{(1-G)(GL^2-1)}}{GL-1} < \pi/2$$

   which tells us that $\cos(nH) > 0$. It follows that

   $$f_{42}(n) = \frac{nL\cos(nH)+\sin(nH)}{n\cos(nH)+\sin(nH)} > 0$$

   .

2. In the case that $G < 1/L$, we have

   $$\pi/2 < \arctan_{[0,\pi]}\frac{\sqrt{(1-G)(GL^2-1)}}{GL-1} < \pi.$$

   which gives us

   $$0 < nH < \arctan_{[0,\pi]}\frac{\sqrt{(1-G)(GL^2-1)}}{GL-1} < \pi.$$

   The range of $0 < nH < \pi/2$ gives $\cos(nH) > 0$ and we do not need to worry about it. However, when $\pi/2 < nH < \arctan_{[0,\pi]}\frac{\sqrt{(1-G)(GL^2-1)}}{GL-1}$, we want to make sure that $nL\cos(nH)+\sin(nH) > 0$ so that $f_{42}(n)$ is greater than 0. Starting with

   $$\pi/2 < nH < \arctan_{[0,\pi]}\frac{\sqrt{(1-G)(GL^2-1)}}{GL-1},$$

we have

$$\frac{\sqrt{(1-G)(GL^2-1)}}{\sqrt{(GL-1)^2+(1-G)(GL^2-1)}} < \sin(nH) < 1$$

and

$$-\frac{1-GL}{\sqrt{(GL-1)^2+(1-G)(GL^2-1)}} < \cos(nH) < 0$$

which leads to

$$-L\sqrt{\frac{GL^2-1}{(1-G)L^2}}\frac{1-GL}{\sqrt{(GL-1)^2+(1-G)(GL^2-1)}} < nL\cos(nH) < 0$$

and

$$nL\cos(nH)+\sin(nH) > \frac{G(L-1)\sqrt{GL^2-1}}{\sqrt{1-G}\sqrt{(GL-1)^2+(1-G)(GL^2-1)}} > 0$$

Since $f_{42}(n)$ is greater than zero in both cases, it follows that $f_4(n)$ is a decreasing functions for $0 < n < \sqrt{\frac{GL^2-1}{(1-G)L^2}}$.

We notice that as $\lambda \to 0$ from the left, $n \to \sqrt{\frac{GL^2-1}{(1-G)L^2}}$ and $m \to \infty$ and we have $f_3(m) = f_4(n) = \frac{1}{L}$. Since both $f_3(m)$ and $f_4(n)$ are continuous in their domain and their range only approach each other at $\lambda = 0$, we conclude that $f_4(n) > f_3(m)$ for $\lambda \in (-2(GL^2-1, 0)$. The condition in Eq. 2.13 cannot be satisfied and there does not exist odd eigenfunction corresponding to negative eigenvalue.

Next, we will examined even eigenfunctions. To analyze the condition for even eigenfunctions in Eq. 2.14, we want to group the functions of $m$ and the functions of $n$ on a separate side of the equation and write:

$$\frac{g_1(m)}{g_2(m)} = \frac{g_1(n)}{g_2(n)}.$$

Note that this is possible because in this range of $\lambda$, $g_2(m) \neq 0$ and $g_2(n) \neq 0$. For convenient reasons, we will substitute $n$ with $ni$ so that we can explain functions of $n$ as functions of real number. Now, the condition for the existence of even eigenfunctions is

$$g_3(m) = g_4(n)$$

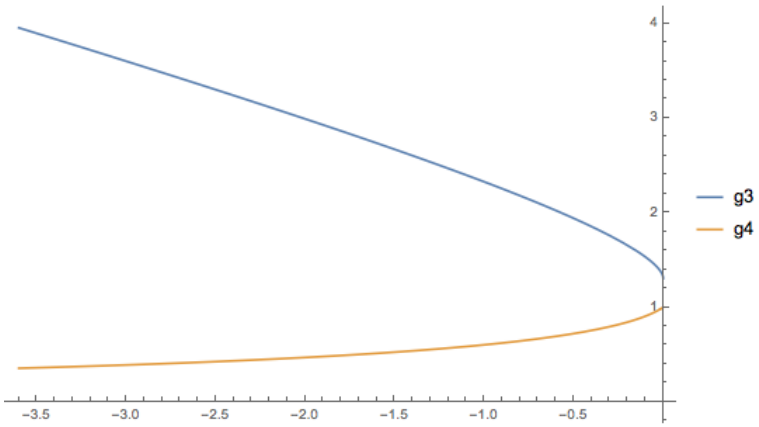


**Figure 2.4** Plot of $g_3(m)$ and $g_4(n)$ as a function of eigenvalue $\lambda \in (-2(GL^2-1), 0)$ with $G = 0.7$ and $L = 2$. (Note that $m$ and $n$ are uniquely determined for each $\lambda$).

where

$$g_3(m) = g_1(m)/g_2(m) = \frac{\left(L^2m^2-1\right)\left(\left((H+1)m^2-1\right)\sinh(Hm)+Hm\cosh(Hm)\right)}{\left(m^2-1\right)\left((Lm^2(H+L)-1\right)\sinh(Hm)+Hm\cosh(Hm))}$$

$$g_4(n) = g_1(ni)/g_2(ni) = \frac{\left(L^2n^2+1\right)\left(\left((H+1)n^2+1\right)\sin(Hn)-Hn\cos(Hn)\right)}{\left(n^2+1\right)\left((HLn^2+L^2n^2+1\right)\sin(Hn)-Hn\cos(Hn))}$$

To prove that the condition $g_3(m) = g_4(n)$ cannot be met, we will show that $g_3(m)$ is a decreasing function while $g_4(n)$ is an increasing function. For example, with $G = 0.7$ and $L = 2$, we can plot $g_3$ and $g_4$ as a function of $\lambda$ in Fig. 2.4.

Let's first examine $g_3'(m)$:

$$g_3'(m) = -\frac{2m(L^2-1)}{(m^2-1)^2}\frac{\left((H+1)m^2-1\right)\sinh(Hm)+Hm\cosh(Hm)}{(Lm^2(H+L)-1)\sinh(Hm)+Hm\cosh(Hm)}$$
$$-\frac{(L^2m^2-1)(L-1)m(H+L+1)}{m^2-1}\frac{\left(2H^2m^2+Hm\sinh(2Hm)-2\cosh(2Hm)+2\right)}{2\left((HLm^2+L^2m^2-1)\sinh(Hm)+Hm\cosh(Hm)\right)^2}.$$

Under the condition that $L > 1$, $m > 1$ and $H > 1$, it is obvious that

$$\frac{\left((H+1)m^2-1\right)\sinh(Hm)+Hm\cosh(Hm)}{(Lm^2(H+L)-1)\sinh(Hm)+Hm\cosh(Hm)} > 0.$$

The less obvious part is to prove that

$$\left(2H^2m^2 + Hm\sinh(2Hm) - 2\cosh(2Hm) + 2\right) > 0$$

which can be done by expanding taylor series of

$$2x^2 + x\sinh(2x) - 2\cosh(2x) + 2$$

at $x = 0$ and observing that the coefficients of all powers are positive. It follows that $g_3'(m) < 0$, so $g_3(m)$ is a decreasing function for $m > 1$.

Next, we want to show that $g_4(n)$ is an increasing function. Remind that

$$\begin{aligned} g_4(n) &= \frac{\left(L^2n^2+1\right)\left(\left((H+1)n^2+1\right)\sin(Hn) - Hn\cos(Hn)\right)}{(n^2+1)\left((HLn^2+L^2n^2+1)\sin(Hn) - Hn\cos(Hn)\right)} \\ &= \frac{\left(L^2n^2+1\right)}{(n^2+1)}\left(1 - \frac{(L-1)n^2(H+L+1)\sin(Hn)}{(HLn^2+L^2n^2+1)\sin(Hn) - Hn\cos(Hn)}\right) \end{aligned}$$

It is not difficult to show that $\frac{\left(L^2n^2+1\right)}{\left(n^2+1\right)}$ is an increasing function. If $G > 1/L$ which implies that $0 < nH < \pi/2$, we know that

$$\frac{\left(\left((H+1)n^2+1\right)\sin(Hn) - Hn\cos(Hn)\right)}{\left((HLn^2+L^2n^2+1)\sin(Hn) - Hn\cos(Hn)\right)} > 0$$

because of the identity $\tan(x) > x$ for $0 < x < \pi/2$. If $G < 1/L$ which implies that $0 < nH < \pi$, the inequality

$$\frac{\left(\left((H+1)n^2+1\right)\sin(Hn) - Hn\cos(Hn)\right)}{\left((HLn^2+L^2n^2+1)\sin(Hn) - Hn\cos(Hn)\right)} > 0$$

still holds because, when $\pi/2 < nH < \pi$, $\cot(nH) < 0$. Now, we just need to show that

$$\frac{\sin(Hn)}{(HLn^2+L^2n^2+1)\sin(Hn) - Hn\cos(Hn)}$$

is a decreasing function to prove that $g_4(n)$ is an increasing function on $0 < n < \bar{\mu}$. We observe that

$$\frac{\sin(Hn)}{(HLn^2+L^2n^2+1)\sin(Hn) - Hn\cos(Hn)} = \left(\left(HLn^2+L^2n^2+1\right) - Hn\cot(Hn)\right)^{-1}$$

where $\left(HLn^2+L^2n^2+1\right)$ and $-Hn\cot(Hn)$ are increasing functions on $0 < nH < \pi$. In conclusion, $g_4(n)$ is an increasing function while $g_3(n)$ is an decreasing function where $g_4(\bar{\mu}) < g_3(\bar{\mu})$, so $g_4(n) < g_3(n)$ for all $0 < n < \bar{\mu}$. The condition for even eigenfunction cannot be satisfied, implying that the eigenvalue cannot have a value between $-2(GL^2 - 1)$ and 0.

### 2.2.4 Eigenvalue cannot be zero

At $\lambda = 0$, the quadratic equation describing the values of $m_*$ (Eq. 2.8) reduces to

$$2(1-G)L^2 m_*^2 + 2(GL^2 - 1) = 0.$$

Thus, the eigenfunction corresponding to $\lambda = 0$ is

$$\widetilde{\rho}(x) = A\sin(mx) + B\cos(mx) + C$$

where $A$, $B$, and $C$ are constants and

$$m = \sqrt{\frac{GL^2 - 1}{L^2(1-G)}}.$$

1. Odd: first, let's look at the odd part of the eigenfunction

   $$\widetilde{\rho}(x) = B\sin(\widetilde{\mu}x)$$

   and plug it into the eigenvalue equation. The coefficients of the modes spanned by $\{\sinh(x), \sinh(x/L)\}$ give the following constraints:

   $$-\frac{A(\sin(Hm) + m\cos(Hm))}{m^2+1} = 0$$
   $$\frac{AGL^2(Lm\cos(Hm) + \sin(Hm))}{L^2m^2+1} = 0$$

   We want a nontrivial solution where $A \neq 0$ which requires that:

   $$\tan(mH) = -m$$
   $$\tan(mH) = -Lm$$

   These two equalities cannot be satisfied simutaneously if $L > 1$. It follows that $A$ has to be zero, and no odd eigenfunctions corresponding to $\lambda = 0$.

2. Even: next, let's look at the even part of the eigenfunction

   $$\widetilde{\rho}(x) = A\cos(mx) + C.$$

First, $\widetilde{\rho}$ must have zero mean so $C = -A\frac{\sin(mH)}{mH}$. We plug this equation of $\widetilde{\rho}$ into the eigenvalue equation. The coefficients of the modes spanned by $\{\cosh(x), \cosh(x/L)\}$ give the following constraints:

$$\frac{Ae^{-H}\left(\left((H+2)m^2+2\right)\sin(Hm) - Hm\cos(Hm)\right)}{Hm\left(m^2+1\right)} = 0$$
$$\frac{Ae^{-H/L}GL^2\left(\left(HLm^2+2L^2m^2+2\right)\sin(Hm) - Hm\cos(Hm)\right)}{Hm\left(L^2m^2+1\right)} = 0$$

We want a nontrivial solution where $A \neq 0$. Suppose for contradiction that $A \neq 0$. It follows that

$$\left(\left((H+2)m^2+2\right)\sin(Hm) - Hm\cos(Hm)\right) = 0$$
$$\left(HLm^2+2L^2m^2+2\right)\sin(Hm) - Hm\cos(Hm) = 0$$

or

$$(L-1)(H+2L+2)m^2\sin(Hm) = 0$$

Since $H = \frac{1}{m}\arctan_{[0,\pi]}\frac{\sqrt{(1-G)(GL^2-1)}}{GL-1}$, the value $\sin(mH)$ cannot be 0 unless $G = 1$ or $GL^2 = 1$. In addition, $L > 1$ and $H > 0$. It follows that $(L-1)(H+2L+2)m^2\sin(Hm) > 0$, creating a contradiction. Thus, the even eigenfunction corresponding to $\lambda = 0$ does not exist neither.

### 2.2.5 At Least One Eigenvalue exists in the range of $\left(0, \frac{2L^2(1-\sqrt{G})^2}{L^2-1}\right)$

In this region, we have that $m$ and $n$ are pure imaginary. We choose to write $m = im$ and $n = in$. It can be shown that

$$\sqrt{\frac{GL^2-1}{(1-G)L^2}} < n < \sqrt{\frac{\sqrt{G}L^2-1}{(1-\sqrt{G})L^2}} < m < \infty$$

(see an example of numerical value of $n$ and $m$ in Fig. 2.1 and 2.2. Substitute $m = im$ and $n = in$ to Eq. 2.13 and get a condition for an odd eigenfunction that

$$F_o(m,n) = f_1(m)f_2(n) - f_2(m)f_1(n) = 0 \tag{2.15}$$

where

$$f_1(\zeta) = \frac{\zeta\cos(\zeta H) + \sin(\zeta H)}{\zeta^2+1},$$
$$f_2(\zeta) = \frac{\zeta L\cos(\zeta H) + \sin(\zeta H)}{\zeta^2L^2+1}.$$

Substitute $m = im$ and $n = in$ to Eq. 2.14 to get a condition for an even eigenfunction that

$$F_e(m,n) = g_1(m)g_2(n) - g_2(m)g_1(n) = 0 \tag{2.16}$$

where

$$g_1(\zeta) = \frac{\zeta H\cos(\zeta H) + (-1 + (1+H)\zeta^2)\sin(\zeta H)}{\zeta^2+1},$$
$$g_2(\zeta) = \frac{\zeta H\cos(\zeta H) + (-1 + L(L+H)\zeta^2)\sin(\zeta H)}{\zeta^2 L^2+1}.$$

There are infinitely many eigenfunctions corresponding to the positive eigenvalues in $\left(0, \frac{2L^2(1-\sqrt{G})^2}{L^2-1}\right)$. For instance, for $G = 0.4, L = 2$, we can plot $F_o$ and $F_e$ over $\lambda$ in Fig. 2.5 and 2.6 respectively.

We want to show that there exists at least one positive eigenfunction corresponding to a positive eigenvalue. Let's look at Eq. 2.15. We can plug in the values of $f_1$ and $f_2$ to obtain that

$$F_o(\lambda) = -\frac{(L-1)\left(-\sin(mH)f_1^*(m,n) + m\cos(mH)f_2^*(m,n)\right)}{(m^2+1)(n^2+1)(L^2m^2+1)(L^2n^2+1)}$$

where

$$f_1^*(m,n) = n\cos(Hn)\left(m^2\left(L^2\left(n^2+1\right)+L+1\right) - Ln^2+1\right) + (L+1)\left(m^2-n^2\right)\sin(Hn)$$

and

$$f_2^*(m,n) = \sin(Hn)\left(L^2\left(m^2+1\right)n^2 + L\left(n^2-m^2\right) + n^2 + 1\right) + L(L+1)n\left(n^2-m^2\right)\cos(Hn).$$

The function $f_1^*$ and $f_2^*$ do not change sign rapidly on $m$. Note that we write $F_o$ as a function of $\lambda$ because $m$ and $n$ are functions of $\lambda$. Since at small positive $\lambda$, $m$ decreases rapidly from infinity while $n$ increases slowly at low value (see Fig. 2.2), there exists some small $\lambda_1$, yielding the pair of $(m_1, n_1)$, and small $\lambda_0$, yielding the pair of $(m_0, n_0)$ such that

$$|m_1 - m_0| = \pi$$
$$|n_1 - n_0| \to 0.$$

We consider some $m_0 = 2\pi Z$ where $Z \in \mathbb{Z}^+$ so that $F_o(m_1, n_1) \approx -F_o(m_0, n_0)$. Since $m$ and $n$ are functions of $\lambda$, by the mean value theorem, there exists

some $\lambda_0 < \lambda_2 < \lambda_1$ such that $F_o(\lambda_2) = \frac{1}{2}\left(F_o(\lambda_0) + F_o(\lambda_1)\right) = 0$. We conclude that there exists at least one eigenfunction corresponding to a positive eigenvalue.

Last but not least, we have proved that eigenvalues cannot be negative or zero, and that some positive eigenvalue exists. Therefore, $\mathcal{L}$ is a positive definite operator, implying that $W_2 = \left\langle \widetilde{\rho}, \mathcal{L}\widetilde{\rho} \right\rangle > 0$. The candidate solution in Eq. 1.7 is globally stable with respect to the perturbation inside the support of the solution.

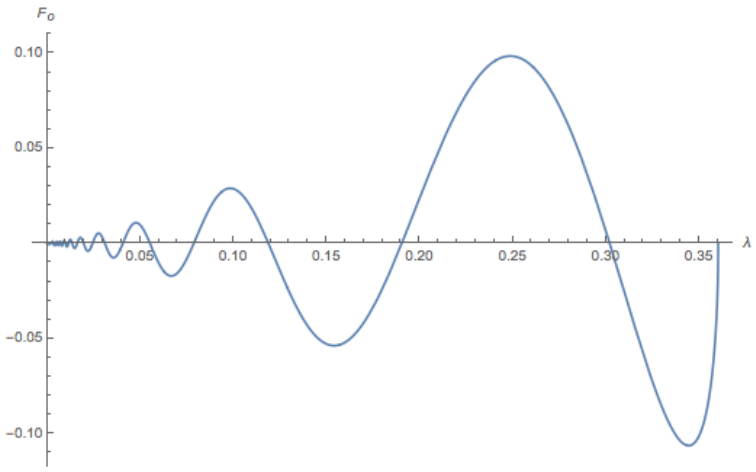


**Figure 2.5** Plot of $F_o$ from $\lambda = 0$ to $\frac{2L^2(1-\sqrt{G})^2}{L^2-1}$ for $G = 0.4, L = 2$. The x-intercepts represent eigenvalues that satisfy the condition which means that the odd eigenfunction corresponding to that eigenvalue exist.

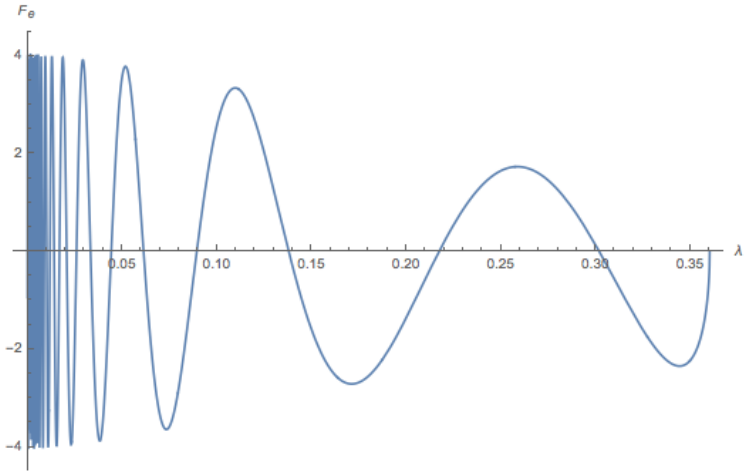


**Figure 2.6** Plot of $F_e$ from $\lambda = 0$ to $\frac{2L^2(1-\sqrt{G})^2}{L^2-1}$ for $G = 0.4, L = 2$. The x-intercepts represent eigenvalues that satisfy the condition which means that the even eigenfunction corresponding to that eigenvalue exist.

## 2.3 A Numerical Method of finding eigenvalues

From the previous chapter, we found that all eigenvalues are positive, but it is in our best interest to verify the result of our finding numerically. Remind that the eigenvalue equation is

$$\mathcal{L}\widetilde{\rho} = \lambda\widetilde{\rho}$$

where $\rho$ is a probability density function of mass 1,

$$\mathcal{L}\tilde{\rho}(x) = \int_{\Omega} \tilde{\rho}(y)\left(Q(x-y) - \frac{\widetilde{Q}(y)}{|\Omega|}\right)dy$$

and

$$\widetilde{Q}(y) = 2(1 - GL^2) - 2e^{-H}\cosh(y) + 2GL^2 e^{-H/L}\cosh(y/L).$$

Since $\mathcal{L}$ is a compact operator, we can approximate it using an $n \times n$ matrix namely $\mathbb{L}$. Divide the boundary $\Omega = [-H, H]$ into $n$ parts. Let $x_i$ represents the center of each part so that

$$x_i = -H + \frac{2H}{n}\left(i - \frac{1}{2}\right)$$

and the element in row $i$, column $j$ of $\mathbb{L}$ is

$$\mathbb{L}_{ij} = \left(Q(|x_i - x_j|) - \frac{\widetilde{Q}(x_j)}{2H}\right)\frac{1}{2H}.$$

We found all eigenvalues of $\mathbb{L}$ numericallly using MATLAB and plotted eigenvalues obtained numerically with eigenvalues analytically from Eq. 2.13 and Eq. 2.14.

The plots in Fig. 2.7(a) and 2.7(b) shows that both analytical approach and numerical approach agree very well with each other that almost all eigenvalues from the two approaches match within 0.1 percent.

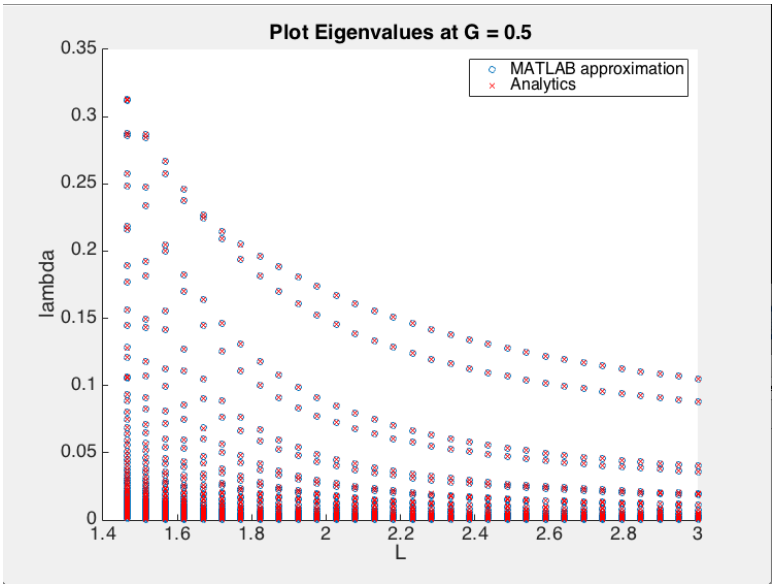


(a) Using $n = 500$, we fix $G = 0.5$ and vary $L$ from $1/\sqrt{G} + 0.05$ to 3

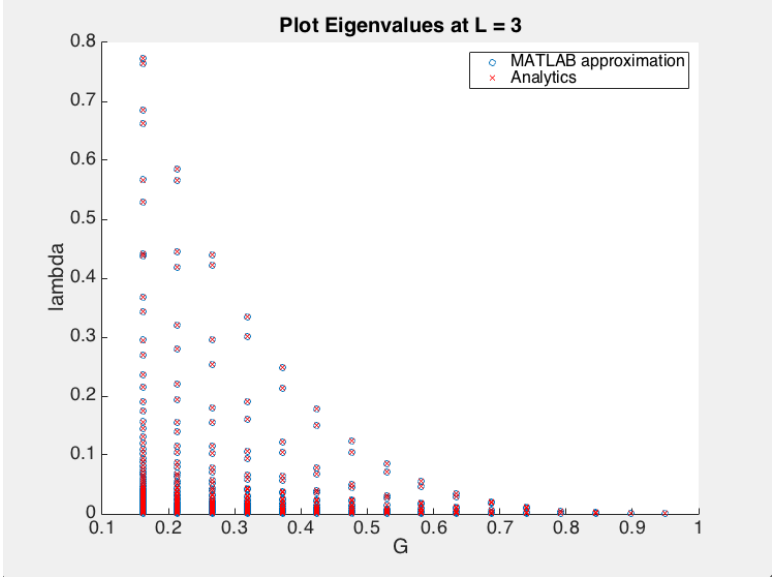


(b) Using $n = 500$, we fix $L = 2$ and vary $G$ from $1/L^2 + 0.05$ to 0.95

**Figure 2.7** Plots comparing eigenvalues calculated from an analytical approach to eigenvalues calculated from a numerical approach.

# Chapter 3

# Convex Relaxation

In the second chapter, we have proved that every probability density function with support smaller than the candidate solution (Eq. 1.7) has higher energy than the candidate solution. We would like to go farther and prove that every probability density function in the real line has higher energy than the candidate solution. In other word, we would like to prove that the candidate solution that we already knew is a local minimum to be a global minimum. First, let's remind that the candidate solution in Eq. 1.7 is

$$\bar{\rho}(x) = \begin{cases} C\cos(\widetilde{\mu}x) + D & , x \in \Omega_{\bar{\rho}} = [-H, H] \\ 0 & , \text{Otherwise} \end{cases} \tag{3.1}$$

where

$$\begin{aligned} \bar{\mu} &= \sqrt{\frac{GL^2 - 1}{L^2(1-G)}}, \\ H &= \frac{1}{\bar{\mu}} \cot^{-1}_{[0,\pi]} \left\{ \frac{GL - 1}{\sqrt{(1-G)(GL^2-1)}} \right\}, \\ C &= \frac{M}{2(H+L+1)} \frac{\sqrt{G}(L^2-1)}{L(1-G)}, \\ D &= \frac{M}{2(H+L+1)}. \end{aligned}$$

We decide to explore an alternative approach of convex relaxation on the pairwise interaction problems, which comes out recently in (Bandegi and Shirokoff, 2015) . Convex relaxation is an idea based on the fact that a

nonlinear problem may contain multiple minimums, but a linear problem in a convex region may only contain one minimum and that minimum must be a global minimum. A local minimum of a non-linear problem may not be a global minimum, but every local minimum of a linear function in a convex space is a global minimum.

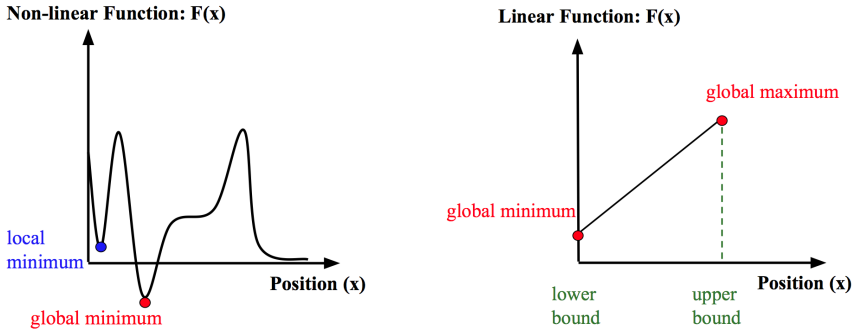


(a) Example of a non-linear function on a real line that has multiple minimums

(b) Example of a linear function on a real line

**Figure 3.1** A local minimum of a non-linear function may not be a global minimum, but a local minimum of a linear function must be a global minimum.

We have a non-linear optimization problem on a convex domain that we would like to find the global minimum. The non-linear function that we are interested is the energy $E$ of the Morse potential system which is a quadratic function of a probablity density function $\rho$:

$$E(\rho) = \frac{1}{2}\int_{\Omega}\int_{\Omega} \rho(x)\rho(y)Q(x-y)dxdy \tag{3.2}$$

such that $\rho(x) \geq 0$ for $x \in \mathbb{R}$ and $\int_{\Omega} \rho(x)dx = 1$ where $\Omega$ is the support of $\rho$. A probability density function is the name for a non-negative function whose integral over the real line equals to 1. The space of probability density function is convex because any linear combination of two probability density functions $\rho_1$ and $\rho_2$ is a probability density function. For $t \in [0,1]$, define $\rho$ as a linear combination of $\rho_1$ and $\rho_2$. We notice that

$$\rho = t\rho_1 + (1-t)\rho_2 \geq 0$$

and

$$\begin{aligned}\int_{-\infty}^{\infty} \rho(x)dx &= \int_{-\infty}^{\infty} \big(t\,\rho_1(x) + (1-t)\rho_2(x)\big)\,dx \\ &= t\int_{-\infty}^{\infty} \rho_1(x)dx + (1-t)\int_{-\infty}^{\infty} \rho_2(x)dx \\ &= t + (1-t) = 1,\end{aligned}$$

which confirm that $\rho$ is a probability density function. Bernoff and Topaz (2013) found a local minimizer of the non-linear optimization problem in Eq. 3.2 analytically using calculus of variations (See Eq. 1.7). Nevertheless, by the nature of the non-linear problem, a local minimum may not necessarily be a global minimum. We hope to change our non-linear problem to a linear one because a local minimum in a linear problem is equivalent to a global minimum.

The study of Bandegi and Shirokoff (2015) suggests that we can acheive this goal by following the two steps. First, transforming the problem from non-linear to linear. Second, relaxing the non-convex domain into a convex one. In the first step, we want to make the energy function in Eq. 3.2 which is a quadratic function of $\rho$ into a linear function. Bandegi and Shirokoff (2015) acheive this by replacing the quadratic term of $\rho$ with a convolution $P(s) = \int_\Omega \rho(x)\rho(x+s)dx$. By substituting $y = x + s$, we observe that the equation for the energy $E$ can be rewritten as a linear function of $P$:

$$\begin{aligned}E(\rho) &= \frac{1}{2}\int_\Omega\int_\Omega \rho(x)\rho(y)Q(x-y)dxdy \\ &= \frac{1}{2}\int_\Omega\int_\Omega \rho(x)\rho(x+s)Q(s)dxds \\ &= \frac{1}{2}\int_{\Omega_p} P(s)Q(s)ds.\end{aligned}$$

where $\Omega_p$ is the boundary of $P$ which differs from $\Omega$. If $\Omega = [-h, h]$ then $\Omega_p = [-2h, 2h]$ because $s = y - x$ and the domain of $x$ and $y$ is $\Omega$.

There is a trade-off when we transform a non-linear function to a linear function; the domain of the problem is no longer convex. A linear problem in a non-covex domain can still maintain multiple minimum, which destroy the purpose of converting to a linear problem in the first place.

In the next step, we want to relax the domain of $P$ to a convex space. This technique is called "convex relaxation." The idea of this technique is to choose a convex space containing our non-convex space and solve the linear

optimization on that convex space instead. The local minimum found in the linear optimization on a convex domain is a global minimum. Thus, if the global minimum obtained lies inside the non-convex domain, then we are fine because after we shrink the domain back to be non-convex the solution is still a global minimum because the original non-convex domain lies inside the convex one. However, if we are unfortunate and the global minimum lies outside the non-convex domain then we cannot make the same conclusion because the space outside our non-convex domain of $P$ is not a valid auto-correlation of a probability density function.

Let denote the domain of $P$ with $\mathcal{A}$:

$$\mathcal{A} = \left\{ P \mid P = \int_{\Omega} \rho(x)\rho(x+s)dx \text{ where } \rho \text{ is a probability density function} \right\}.$$

Several convex spaces can contain $\mathcal{A}$, for instance, the convex hull of $\mathcal{A}$, but if we choose this smallest convex domain it may prove difficult to find its boundary. In addition, choosing a large convex domain may cause the global minimum to lie outside $\mathcal{A}$. Choosing the right convex domain that contains $\mathcal{A}$ seems to be an art rather than science. Without lose of generality, let's look at the fourier transform of

$$\rho(x) = \frac{a_0}{2} + \sum_{n=1}^{\infty} \left( a_n \cos(k_n x) + b_n \sin(k_n x) \right).$$

Thus, $P$, the auto-correlation of $\rho$, is

$$\begin{aligned} P &= \int_{\Omega} \rho(x)\rho(x+s)\, dx \\ &= \frac{a_0^2}{4} + \sum_{n=1}^{\infty} \left( a_n^2 + b_n^2 \right) \cos(k_n x). \end{aligned}$$

Notice that the sin terms go away, leaving only the cos terms with coefficient $a_n^2 + b_n^2 \geq 0$. So, it seems natural that the study of Bandegi and Shirokoff (2015) suggests the convex cone of non-negative Fourier cosine modes. Let's call this convex cone:

$$\mathcal{B} = \{ P : \langle P, \cos(2\pi \mathbf{k} \cdot \mathbf{x} \rangle \geq 0, P(-x) = P(x) \geq 0, \text{ and } \int_{\Omega_p} P(x)\, dx = 1 \}$$

where $k = 2m\pi/|\Omega|$ for $m \in \mathbb{Z}^+$ and $\langle f(x), g(x) \rangle = \int_{\Omega_p} f(x)g(x)\, dx$.

## 3.1 Periodic Boundary Condition

Before running the numerical simulation, we need to transform our Morse potential to a periodic Morse potential. We need a periodic potential because numerical simulation can only be done in a bounded domain, so we need to make the domain periodic. Let's consider a periodic domain in $\mathbb{R}$ on $[-h, h]$. We can transform Morse potential ($Q$) to periodic Morse potential ($Q_p$) using the following formula:

$$Q_p(z) = \sum_{n=-\infty}^{\infty} Q(z + 2nh).$$

where $z = x - y$ is the displacement from one animal at position $y$ to the other animal at position $x$. The summation of $Q(z+2nh)$ represents the sum of all forces of the animal in position $y$ causes. The term $2nh$ represents the multiple length of the periodic interval. The particle living at position $y$ is equivalent to the particle living at position $2h + y$, $4h + y$, ..., $2nh + y$ for all integer $n$. This summation leads to

$$\begin{aligned}
Q_p(z) &= \sum_{n=-\infty}^{\infty} Q(z + 2nh) \\
&= \sum_{i=-\infty}^{\infty} e^{-|z+2nh|} - GLe^{-|z+nh|/L} \\
&= e^{-|z|} - GLe^{-|z|/L} + \sum_{i=1}^{\infty} e^{-(z+2ih)} - GLe^{-(z+nh)/L} + \sum_{n=-\infty}^{-1} e^{z+2nh} - GLe^{(z+nh)/L} \\
&= e^{-|z|} - GLe^{-|z|/L} + \frac{e^{z} + e^{-z}}{e^{2h} - 1} - GL\frac{e^{z/L} + e^{-z/L}}{e^{2h/L} - 1} \\
&= \frac{\cosh(|z| - h)}{\sinh(h)} - GL\frac{\cosh((|z| - h)/L)}{\sinh(h/L)}.
\end{aligned}$$

This periodic Morse potential becomes the usual Morse potential when $h \to \infty$. The plot of this potential for $G = 0.4$, $L = 2$, and $h = 5$ is shown in Fig 3.2. Using the calculus of variations on the first variation of the energy, $W_1$ in Eq. 2.3, similar to how Bernoff and Topaz (2013) solve for the candidate solution of the system under $Q$, we obtain the condition for the candidate solution of the system under $Q_p$ to be

$$\lambda_p = \int_{\Omega} \bar{\rho}_p(x) Q_p(x - y)\, dy \tag{3.3}$$

where $\lambda$ is a constant. Define the differential operators $\mathcal{L}_1 \equiv \partial_{xx} - 1$ and $\mathcal{L}_2 \equiv L^2\partial_{xx} - 1$. We apply $\mathcal{L}_1\mathcal{L}_2$ to Eq. 3.3 to obtain

$$\lambda_p = -2L^2(1-G)(\bar{\rho}_p)_{xx} - 2(GL^2-1)\bar{\rho}_p.$$

This equation yields a candidate solution similar to the candidate solution of Morse potential:

$$\bar{\rho}_p(x) = \begin{cases} C_p \cos(\bar{\mu}x) + D_p & , x \in \Omega_{\bar{\rho}_p} = [-H_p, H_p] \\ 0 & , \text{Otherwise} \end{cases} \tag{3.4}$$

where $H_p$, $C_p$, and $D_p$ can be obtained analytically, and $\bar{\mu} = \sqrt{\frac{GL^2-1}{L^2(1-G)}}$ is the same parameter we have for Eq. 1.7. We can solve for $H_p$ using the implicit equation,

$$\cot(H_p\bar{\mu}) = \frac{\left(\bar{\mu}^2+1\right)\left(L^2\bar{\mu}^2+1\right)\left(\frac{L\bar{\mu}\left(e^{2H_p}-e^{2h}\right)\left(e^{\frac{2h}{L}}+e^{\frac{2H_p}{L}}\right)}{L^2\bar{\mu}^2+1} + \frac{\bar{\mu}\left(e^{2h}+e^{2H_p}\right)\left(e^{\frac{2h}{L}}-e^{\frac{2H_p}{L}}\right)}{\bar{\mu}^2+1}\right)}{\left(L^2-1\right)\bar{\mu}^2\left(e^{2h}-e^{2H_p}\right)\left(e^{\frac{2h}{L}}-e^{\frac{2H_p}{L}}\right)}.$$

Notice that if we divide the numerator and the numerator on the right hand side with $e^{2h+2h/L}$ and let $e^{2(H_p-h)}$ and $e^{2(H_p-h)/L}$ go to zero when $h \to \infty$, then we obtain

$$H_p = \frac{1}{\bar{\mu}}\cot^{-1}_{[0,\pi]}\left\{\frac{GL-1}{\sqrt{(1-G)(GL^2-1)}}\right\},$$

which is identical to $H$ the support of the candidate solution under the normal Morse potential in the infinite domain. The equations for $C_p$ and $D_p$ are

$$C_p = \frac{\bar{\mu}\left(\bar{\mu}^2+1\right)}{2\left(1+\left(\bar{\mu}^2\left(\frac{H_p\left(e^{2h}+e^{2H_p}\right)}{e^{2h}-e^{2H_p}}+1\right)\right)\sin\left(\bar{\mu}H_p\right)-\bar{\mu}H_p\cos\left(\bar{\mu}H_p\right)\right)}, \text{ and}$$

$$D_p = \frac{m\left(\cos(Hm) - \frac{m\left(e^{2h}+e^{2H}\right)\sin(Hm)}{e^{2h}-e^{2H}}\right)}{2\left(Hm\cos(Hm) - \left(\frac{Hm^2\left(e^{2h}+e^{2H}\right)}{e^{2h}-e^{2H}}+m^2+1\right)\sin(Hm)\right)}$$

which reduce to $C$ and $D$, the parameters for Eq. 3.1, as $h \to \infty$.

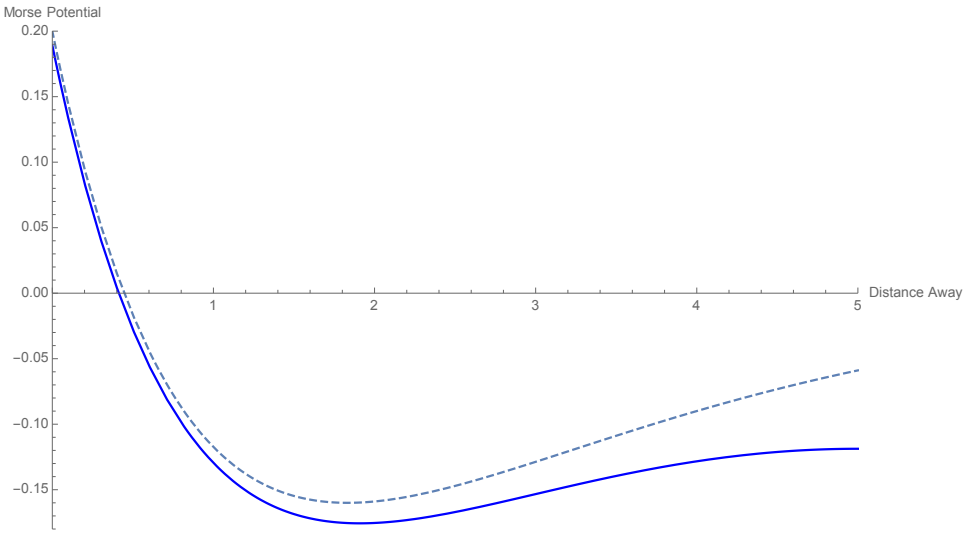


**Figure 3.2** The solid line is the plot of periodic Morse potential and the dashed line is the plot of Morse potential. The parameter $G = 0.4$, $L = 2$, and $h = 5$.

## 3.2 Numerical Scheme

We want to set up a linear optimization problem on a convex domain. There are several linear programming scheme that can gives us the answer numerically. We are interested in the global minimum of the system in an infinite domain, but the numeric can only be done in a finite domain. So, we will use the periodic Morse potential to calculate the interaction in the numeric, and increase the boundary large enough that the periodic Morse potential comes close to the normal Morse potential. We let the boundary of the numerical scheme be $\bar{\Omega} = [-\bar{H}, \bar{H}]$ such that $\bar{H} \approx 10H_p$. We want to perform a linear optimization of

$$E[P(z)] = \frac{1}{2}\int_{\bar{\Omega}} P(z)Q(z)\,dz$$

with the constraints that $P \in \mathcal{B}$ where

$$\mathcal{B} = \{P : \langle P, \cos(2\pi\mathbf{k}\cdot\mathbf{x}\rangle \geq 0, \langle P, \sin(2\pi\mathbf{k}\cdot\mathbf{x}\rangle = 0, P(x) \geq 0, \text{ and } \int_{\Omega} P(x)dx = 1\}$$

where $k = 2m\pi/|\Omega|$ for $m \in \mathbb{Z}^+$. The constraints in $\mathcal{B}$ lead to 3 conditions:

1. $P(z) \geq 0$
2. $\int_{\bar{\Omega}} P(z)\, dz = 1$
3. $c_m = \int_{\bar{\Omega}} P(z)\cos(k_m z)dz \geq 0$ where $k_m = m\pi/\bar{H}$ for all $m = 1..N$.

To perform numerical calculation, we define the discrete domain $z_j = j\Delta z$ for $j = 0..N$ where $\Delta z = \bar{H}/N$. Next, for convenient, we denote $P_j = P(z_j)$ and $Q_j = Q(z_j)$. Under these notations, the energy of the system becomes

$$E = \frac{\bar{H}}{N}\left(P_0Q_0 + P_NQ_N + 2\sum_{j=1}^{N-1} P_jQ_j\right).$$

Similarly, the three constraints lead to:

1. $P_j \geq 0$
2. $1 = \frac{\bar{H}}{N}\left(P_0 + P_N + 2\sum_{j=1}^{N-1} P_j\right)$
3. $0 \geq c_m = \frac{\bar{H}}{N}\left(P_0 + (-1)^m P_N + 2\sum_{j=1}^{N-1} P_j \cos(mj\pi/N)\right)$ for all $m = 1..N$

We use these conditions to perform linear programming problem in MATLAB. Next, we compare the $P$ from linear programming with the $P$ calculated from the auto-correlation of the candidate solution

$$P(s) = \int_{-\infty}^{\infty} \rho(x)\rho(x+s)\, dx$$

where $\rho$ is from Eq. 1.7.

The result of the linear optimization gives us a relatively close solution. The $P$ obtained from the linear programming only differs from the analytical $P$ about 0.1 percent. Since a local minimum in the linear optimization problem is a global minimum and the space of the non-negative Fourier cosin modes is contained in the space of auto-correlation, the local minimizer in the linear optimization implies the global minimizer in the original energy minimization problem. The numerical result suggests that the candidate solution really is a global minimum solution.

## 3.3 Global Minimum with a single component

We want to argue that a single-component local minimizer whose support is larger than the support of the candidate solution in Eq. 1.7 has higher

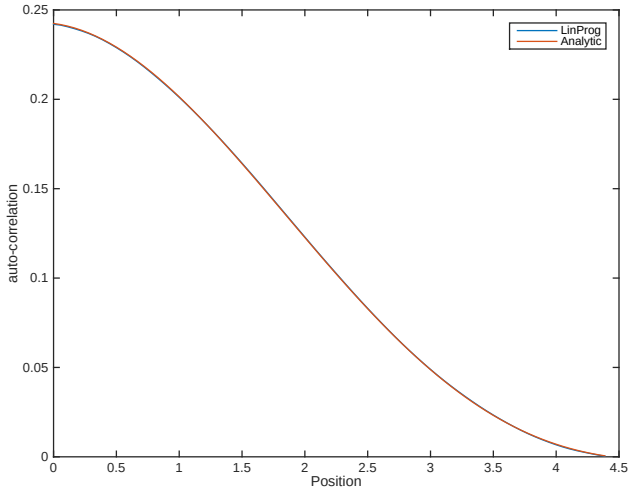


**Figure 3.3** Comparison between the $P$ from linear programming and from the auto-correlation of the candidate solution where $G = 0.5$, $L = 2$, $h = 10$, and the number of grids = $400$.

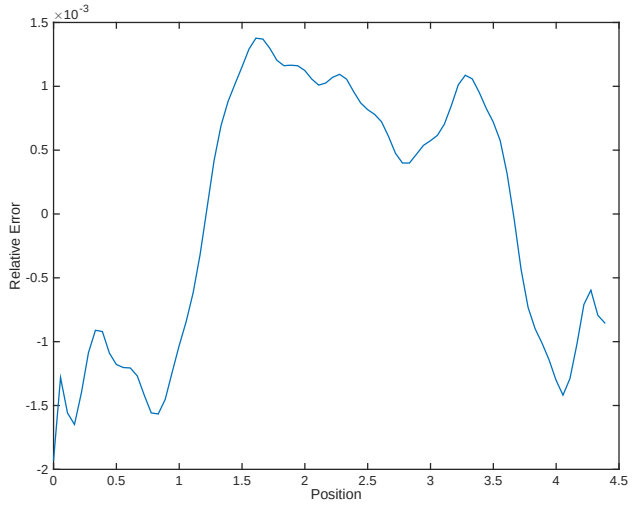


**Figure 3.4** Relative errors of the comparison in Fig. 3.3, $\frac{P_{\text{linprog}} - P_{\text{analytic}}}{\max(P_{\text{analytic}})}$, where $G = 0.5$, $L = 2$, $h = 10$, and the number of grids = $400$.

energy. Let's $\Omega$ be the support of the candidate solution $\rho$ from $[-H, H]$ and $\Omega'$ be the support of a larger local minimizer $\rho'$ from $[-H', H']$ where $H' > H > 0$. Since $\Omega \subset \Omega'$, we can put the candidate solution inside a larger local minimizer. Consider the interaction energy between the two minimizers of mass 1:

$$W(\rho, \rho') = \int_{\Omega} \int_{\Omega'} \rho(x)\rho'(y)Q(x-y)dxdy$$

Let's define $\Lambda(x) = \int_{\Omega} \rho(y)Q(x-y)dy$ be the potential due to $\rho$ and, similarly, $\Lambda'(x) = \int_{\Omega'} \rho'(y)Q(x-y)dy$. We observe that there are two ways to evaluate $W(\rho, \rho')$. In the first way, we evaluate $W = \int_{\Omega} \Lambda'(x)\rho(x)dx = \lambda'$ where $\lambda'$ is equal to the energy of $\rho'$ interacts with itself. In the second way, we evaluate $W = \int_{\Omega} \Lambda(x)\rho(x)dx$. Since the candidate solution is locally minimized $\Lambda(x) > \lambda$ for $x$ outside $\Omega$. So, $W > \lambda$. The calculation from both ways must be equivalent, so $\lambda' > \lambda$. Thus, if there exists a single-component local minimizer of a size larger than $2H$ then its energy will be larger than $\lambda$. This means that a single-component global minimizer must have a size less than or equal to $2H$. However, since we have proved earlier that the candidate solution is globally stable to any perturbation inside the support $[-H, H]$, the candidate solution must be a global minimizer of a single-component solution.

# Chapter 4

# Conclusion and Future Work

In chapter 2, we proved that the candidate solution in Eq. 1.7 has the least energy compared to any state with smaller size. Ultimately, we would like to show that this solution has the least energy compared to any state on the real line, but the calculus of variations seems insufficient because the condition $\rho \geq 0$ restricts allowed perturbations outside of the support of the solution.

Numerically, the chapter 3 provides a convincing evidence that the candidate solution is or close to the solution with globally minimum energy regard to any perturbation in the real line. The energy of the candidate solution for some particular parameters differs 1 in 1000 from the numerical solution.

With a thought experimental in the section 3.3, we were able to rule out the possibility of a global minimizer with a single-component support that is large than $\Omega = [-H, H]$ of the candidate solution in Eq. 1.7. For future work, we only need to prove that a solution with multi-component support where each support is smaller than $\Omega$ has higher energy than the candidate solution.

# Bibliography


Bandegi, Mahdi, and David Shirokoff. 2015. Approximate global minimizers to pairwise interaction problems approximate global minimizers to pairwise interaction problems via convex relaxation. *ArXiv e-prints* .

Bernoff, Andrew J., and Chad M. Topaz. 2013. Nonlocal aggregation models: A primer of swarm equilibria. *SIAM Journal on Applied Dynamical Systems* 55(4):709–747.

Bodnar, M., and J. J. L. Velasquez. 2005. Derivation of macroscopic equations for individual cell- based models: A formal approach,. *Math Methods Appl Sci* 28:1757–1779.

———. 2006. An integro-differential equation arising as a limit of individual cell-based models. *J Differential Equations* 222:341–380.

Breder, C. M. 1954. Equations descriptive of fish schools and other animal aggregations. *Ecology Society of America* 35(3):361–370.

d'Orsogna, M. R., Y. L. Chuang, A. L. Bertozzi, and L. Chayes. 2006. Self-propelled particles with self-propelled particles with soft-core interactions: Patterns, stability, and collapse. *Phys Rev Lett* 96.

Eftmie, R., G. de Vries, and M. A. Lewis. 2007. Complex spatial group patterns result from different complex spatial group patterns result from different animal communication mechanisms. *PNAS* 104(17).

Leverentz, Andrew J., Chad M. Topaz, and Andrew J. Bernoff. 2009. Asymptotic dynamics of attractive-repulsive swarms. *SIAM Journal on Applied Dynamical Systems* 8(3):880–908.

Mogilner, A., L. Edelstein-Keshet, L. Bent, and A. Spiros. 2003. Mutual interactions, potentials, and individual distance in a social aggregation. *J Math Biol* 47(353-389).

Mogilner, A., and X. Yang. 1999. A non-local model for a swarm. *J Math Biol* 38:534–570.

Porter, David, and David S. G. Stirling. 1990. *Integral equations: a rigorous and practical treatment*. Cambridge University Press.